

## Charge-Transfer Complexes of PXX (PXX = 6, 12-Dioxaanthanthrene). The Formal Charge and Molecular Geometry

Takehiro Asari, Norihito Kobayashi, Toshio Naito, and Tamotsu Inabe\*

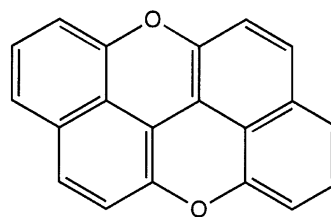
Division of Chemistry, Graduate School of Science, Hokkaido University, Sapporo 060-0810

(Received August 11, 2000)

Three kinds of charge-transfer (CT) complexes of PXX (PXX = 6, 12-dioxaanthanthrene) have been newly prepared and structurally characterized. In the 1:2 CT complex with TNP (TNP = 2,4,6-trinitrophenol), PXX is practically neutral. In the semiconducting partially oxidized salt with  $I_3$ , the PXX molecules form a trimer and each PXX is formally oxidized by  $e/3$ . In the 3:2 salt with  $[Ni(mnt)_2]^-$  (mnt = maleonitriledithiolate), the PXX molecules again form a trimer unit and each PXX is formally oxidized by  $2e/3$ . Together with the structural data obtained from the PXX single component crystal, the molecular geometry change by the formal charge on PXX has been examined. A noticeable change has been found in the aromatic ring framework, which is consistent with the distribution of the HOMO coefficients obtained from the extended Hückel calculation.

The degree of charge transfer in CT complexes of  $\pi$ -conjugated donors and/or acceptors is important for understanding their chemical and physical properties. This information may be obtained from measurements of the infrared spectra; the spectrum becomes the superimposition of the component spectra when the components are neutral, while it changes dramatically when the components are ionized. When the component molecules become  $\pi$ -radicals by removal of an electron from the HOMO orbital or by addition of an electron to the LUMO orbital, the bond strength should be changed according to the population of the HOMO or LUMO coefficients on the bond, producing shifts of the vibrational frequencies. However, this method is applicable only when the molecule has a specific band which is sensitive to the formal charge and is distinguishable from the other bands. On the other hand, the molecular geometry is known to be sensitive to the formal charge on the molecule, and for example, this relationship is well established for TCNQ and is widely used for evaluation of the degree of ionization.<sup>1</sup>

Though the vibrational frequency and molecular geometry are convenient probes for determining the formal charge on molecules, the available data are rather limited. For the title molecule, PXX shown in Chart 1 (this abbreviation comes from its informal name; *peri-xanthenoxanthene*), data are few; only one piece of structural information on the TCNQ complex has been reported.<sup>2</sup> Recently, we have found that PXX can form a highly conducting 1:1 complex with  $[Co^{III}(Pc)(CN)_2]$  (dicyano(phthalocyaninato)cobalt(III)), in which the  $[Co^{III}(Pc)(CN)_2]$  units form a ladder chain.<sup>3</sup> For such a ladder-chain conductor, the electronic structure should strongly depend on the position of the Fermi level. Information about this comes from the degree of charge transfer. The Pc framework is rather insensitive to the charge,<sup>4</sup> and thus the structural data for PXX



PXX  
Chart 1.

are necessary. Therefore, we have intended to determine the crystal structures in which PXX takes various formal charges. We have carried out the crystal growth by combining with various acceptors including very weak ones and that by the electrochemical oxidation using various counter ions. For the neutral species, we have also tried an X-ray structure analysis of the single component PXX crystal. Since PXX is a rather weak donor (the redox potential for the first oxidation is +0.79 V vs.  $Ag/Ag^+$  in acetonitrile), it is relatively difficult to obtain crystals in which the formal oxidation state of PXX is more than +1/2. The crystals obtained so far are  $[PXX][TNP]_2$ ,  $[PXX]_3I_3$ , and  $[PXX]_3[Ni(mnt)_2]_2$ . In this paper we describe their crystal structures, along with that of the single component PXX crystal, and some of their physical properties.

### Experimental

**Materials.** PXX was prepared by a slight modification of the reported method.<sup>5</sup> 1,1'-Bi-2-naphthol was dissolved in an aqueous NaOH solution; then an aqueous  $Cu(CH_3COO)_2$  solution was added. After stirring for 1 hour the solid products were filtered out and dried in a vacuum. PXX was isolated by fractional sublimation and finally purified by vacuum sublimation. TNP was pur-

chased and recrystallized from ethanol.  $\text{Bu}_4\text{N}[\text{Ni}(\text{mnt})_2]$  was prepared following the method reported.<sup>6</sup> When the single crystals of PXX were grown from the solution, it was not possible to complete the X-ray structure analysis due to the anomalously uneven unit cell.<sup>7</sup> Crystal growth by vacuum sublimation was found to give a polymorph which is suitable for the diffraction study. Single crystals of  $[\text{PXX}][\text{TNP}]_2$  were grown by slow cooling and prolonged slow evaporation of a saturated  $\text{CHCl}_3$  solution. Single crystals of  $[\text{PXX}]_3\text{I}_3$  were obtained by electrochemical oxidation of PXX in acetonitrile with  $\text{Bu}_4\text{N}\cdot\text{I}_3$  as an electrolyte. Single crystals of  $[\text{PXX}]_3[\text{Ni}(\text{mnt})_2]_2$  were obtained by electrochemical oxidation of PXX in a chloroform/acetonitrile mixed solvent with  $\text{Bu}_4\text{N}[\text{Ni}(\text{mnt})_2]$  as an electrolyte. The crystals were obtained only when the applied current is relatively high (ca. 10  $\mu\text{A}$ ).

**Measurements.** Electrical-conductivity measurements were carried out using a four-probe method for low-resistance samples and a two-probe method for high-resistance samples. The infrared spectra were recorded on a Perkin–Elmer 1650 FT-IR spectrometer. The visible-near-IR (vis-NIR) spectra were recorded on a JASCO V-570 spectrometer. For the solid sample, the diffuse reflectance diluted with KBr was measured. The spectra were then plotted using the Kubelka–Munk function.

**X-ray Structure Analyses.** An automated Rigaku AFC-7R diffractometer (PXX,  $[\text{PXX}][\text{TNP}]_2$ , and  $[\text{PXX}]_3\text{I}_3$ ) or a Rigaku R-Axis Rapid area detector ( $[\text{PXX}]_3[\text{Ni}(\text{mnt})_2]_2$ ) with graphite-monochromated Mo  $K\alpha$  radiation ( $\lambda = 0.71073 \text{ \AA}$ ) was used for data collection. The data were corrected for Lorentz and polarization effects, and an absorption correction was applied for  $[\text{PXX}]_3\text{I}_3$  and  $[\text{PXX}]_3[\text{Ni}(\text{mnt})_2]_2$ . In all the measurements, no intensity decay was observed. The data-collection conditions and crystal data are summarized in Table 1. The crystal structures were solved by a direct method (SIR 92<sup>8</sup>), and the positions of all the hydrogen atoms were placed at the calculated ideal positions. A full-matrix least-squares technique (teXsan<sup>9</sup>) with anisotropic thermal parameters for non-hydrogen atoms and isotropic ones for hydrogen atoms (1.2 times of the attached carbon) was employed for a structure refinement.<sup>10</sup>

Crystallographic data have been deposited at the CCDC, 12 Union Road, Cambridge CB2 1EZ, UK and copies can be obtained

on request, free of charge, by quoting the publication citation and the deposition numbers 151672–151675.

## Results and Discussion

**Crystal Structure of PXX.** The crystal structure of the single component PXX crystal obtained from vacuum sublimation is shown in Fig. 1. Molecular packing in this crystal may be regarded as a slight modification of those in polycyclic aromatic hydrocarbons. The PXX molecules form a one-dimensional column along the  $b$  axis with slipped stacking. The chain arrangement along the  $c$  axis is a herringbone type, while that along the  $a$  axis occurs by a parallel shift. Interplanar distance is 3.36  $\text{\AA}$ , and there are no specific contacts between the one-dimensional columns.

**Infrared and Vis-NIR Spectra of  $[\text{PXX}][\text{TNP}]_2$ .** The obtained black crystal is expected to have a neutral ground state, since the difference of the redox potentials between the first oxidation of PXX and the first reduction of TNP is large ( $\Delta E_{\text{redox}} = 1.14 \text{ V}$ ) and far from the neutral-ionic boundary.<sup>11</sup> This expect-

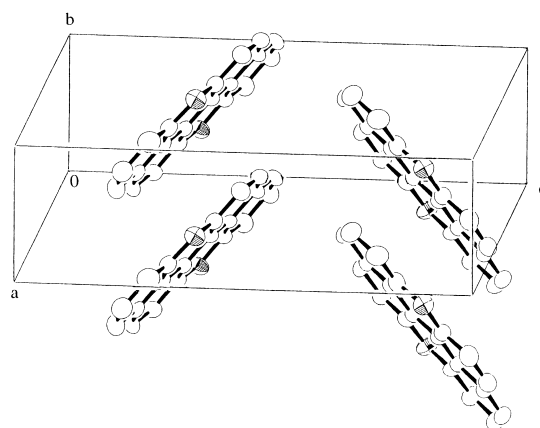


Fig. 1. Crystal structure of PXX.

Table 1. Data-Collection Conditions and Crystal Data

	PXX	$[\text{PXX}][\text{TNP}]_2$	$[\text{PXX}]_3\text{I}_3$	$[\text{PXX}]_3[\text{Ni}(\text{mnt})_2]_2$
Chemical formula	$\text{C}_{20}\text{H}_{10}\text{O}_2$	$\text{C}_{32}\text{H}_{13}\text{N}_6\text{O}_{16}$	$\text{C}_{60}\text{H}_{30}\text{O}_6\text{I}_3$	$\text{C}_{76}\text{H}_{30}\text{N}_8\text{O}_6\text{S}_8\text{Ni}_2$
Formula weight	282.30	737.49	1227.61	1525.00
Crystal size/ $\text{mm}^3$	$0.70 \times 0.30 \times 0.20$	$0.70 \times 0.75 \times 0.10$	$0.10 \times 0.10 \times 0.60$	$0.75 \times 0.50 \times 0.45$
Temperature/K	295	295	295	295
Crystal system	monoclinic	monoclinic	triclinic	triclinic
Space group	$Cc$	$P2_1/n$	$P\bar{1}$	$P\bar{1}$
$a/\text{\AA}$	15.928(3)	7.257(5)	10.595(3)	14.422(1)
$b/\text{\AA}$	4.983(3)	26.267(8)	12.833(2)	15.066(1)
$c/\text{\AA}$	16.170(3)	8.010(4)	8.586(2)	7.448(1)
$\alpha/\text{deg}$			92.56(2)	95.10(1)
$\beta/\text{deg}$	91.33(2)	106.08(4)	112.96(2)	95.42(1)
$\gamma/\text{deg}$			83.39(2)	73.24(1)
$V/\text{\AA}^3$	1283.0(8)	1467(1)	1067.8(5)	1539.4(2)
$Z$	4	2	1	1
$\mu(\text{Mo } K\alpha)/\text{cm}^{-1}$	0.94	1.38	22.57	9.51
No. of reflections measured	1478	3711	5170	6951
No. of reflections observed	1059 [ $I > 2.5\sigma(I)$ ]	2352 [ $I > 3.0\sigma(I)$ ]	3454 [ $I > 3.0\sigma(I)$ ]	5574 [ $I > 3.0\sigma(I)$ ]
$R$	0.042	0.047	0.032	0.036
$R_w$	0.041	0.049	0.028	0.036

tation has been confirmed from the infrared spectra. Figures 2(a), 2(b), and 2(d) show the IR spectra of PXX, TNP, and  $[\text{PXX}][\text{TNP}]_2$ , respectively. The last spectrum is well reproduced by superimposition of the first two spectra. From this result, the formal charge of PXX is reasonably assigned to be 0. The vis-NIR spectra shown in Fig. 3 also clearly support this assignment. The bands in the visible region of the spectrum of  $[\text{PXX}][\text{TNP}]_2$  well correspond to the absorption bands of PXX. The position of the charge-transfer band, around  $15000\text{ cm}^{-1}$  (1.86 eV), is also in good agreement with the simple model proposed by Torrance,<sup>11</sup> and supports the suggestion that this complex is located deep inside the neutral ground state region. The crystal is practically an insulator ( $\rho > 10^8\ \Omega\text{ cm}$  at room temperature).

**Crystal Structure of  $[\text{PXX}][\text{TNP}]_2$ .** As shown in Fig. 4, the crystal comprises  $[\text{TNP}]-[\text{PXX}]-[\text{TNP}]$  trimer units. These units form a pseudo body-centered lattice. There are several short contacts within the face-to-face overlapped trimer (interplanar distance, 3.31 Å), and the intermolecular interaction is in the range of typical charge-transfer complexes with a neutral ground state. The hydroxy group forms an intramolecular hydrogen bond with one of the nitro groups in the

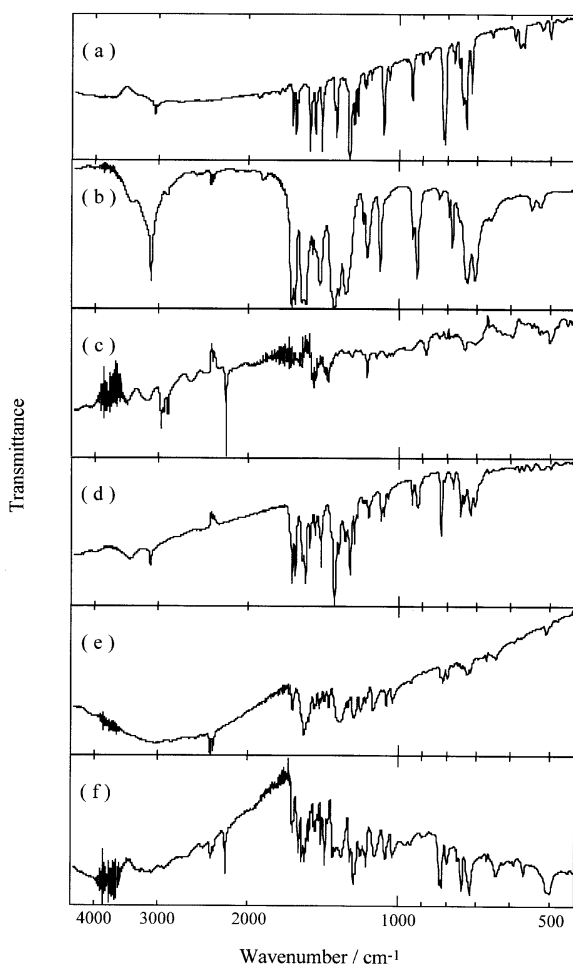


Fig. 2. Infrared spectra of PXX (a), TNP (b),  $\text{Bu}_4\text{N}[\text{Ni}(\text{mnt})_2]$  (c),  $[\text{PXX}][\text{TNP}]_2$  (d),  $[\text{PXX}]_3\text{I}_3$  (e), and  $[\text{PXX}]_3[\text{Ni}(\text{mnt})_2]_2$  (f).

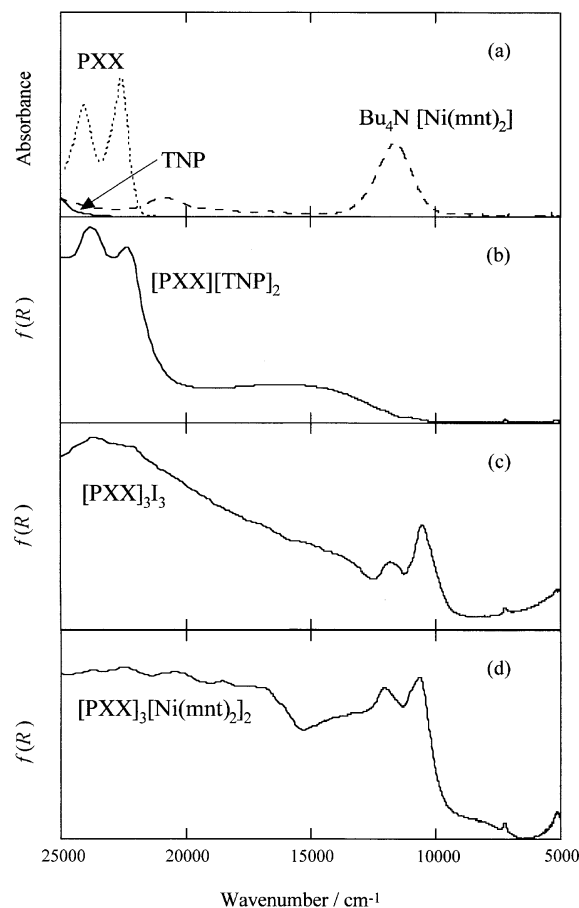
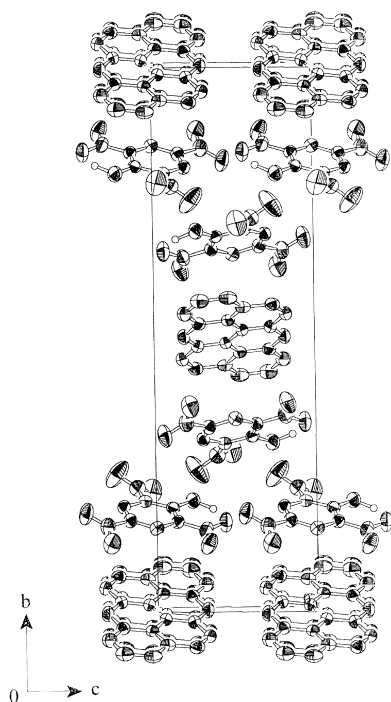


Fig. 3. Vis-NIR spectra of PXX, TNP, and  $\text{Bu}_4\text{N}[\text{Ni}(\text{mnt})_2]$  in each chloroform solution (a), diffuse reflectance spectra plotted by the Kubelka-Munk function,  $f(R)$ , of  $[\text{PXX}][\text{TNP}]_2$  (b),  $[\text{PXX}]_3\text{I}_3$  (c), and  $[\text{PXX}]_3[\text{Ni}(\text{mnt})_2]_2$  (d).

same molecule, and does not participate in the intermolecular hydrogen bonding.

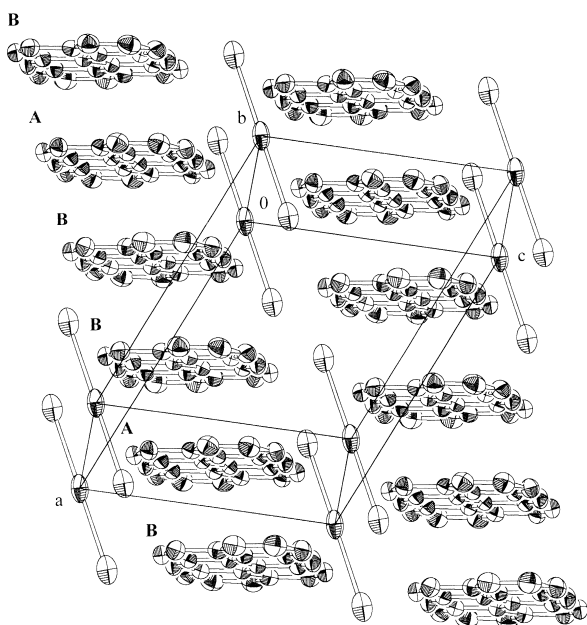
**Infrared and Vis-NIR Spectra and Electrical Conductivity of  $[\text{PXX}]_3\text{I}_3$ .** Since this compound is a partially oxidized salt, the fractional charge can be estimated from the stoichiometry. The iodine atoms are observed as a discrete trihalide anion (vide infra), so the formal charge is estimated to be  $+1/3$ . Some information on whether the charge is distributed uniformly or disproportionately may be obtained from the optical and electrical measurements. The infrared spectrum of  $[\text{PXX}]_3\text{I}_3$  is shown in Fig. 2(e). There are vibrational bands most of which are not coincide with the bands observed for neutral PXX in Fig. 2(a), in addition to the broad electronic absorption band. This feature is characteristic of partially oxidized salts in which the charge delocalization occurs. Indeed, the crystal is conducting;  $\rho_{\text{RT}} = 10^2\ \Omega\text{ cm}$  with the activation energy of 0.19 eV, which is in good agreement with the gap energy estimated from the electronic transition in the IR region.

The vis-NIR spectrum is considerably different from that of  $[\text{PXX}][\text{TNP}]_2$ , as shown in Fig. 3(c). There are extra bands around  $11000\text{ cm}^{-1}$ , which may be assigned to the intramolecular electronic transition in the PXX cation radical.

Fig. 4. Crystal structure of [PXX][TNP]<sub>2</sub>.

**Crystal Structure of [PXX]<sub>3</sub>I<sub>3</sub>.** In this crystal, there are two crystallographically independent PXX's; one molecule (molecule A) lies on the inversion center and the other (molecule B) is located at the general position. The molecular geometry is not so much different for these two molecules (*vide infra*). This is consistent with the optical and electrical properties, and the charge is assumed to be delocalized to some extent.

The crystal structure is shown in Fig. 5. The crystal is com-

Fig. 5. Crystal structure of [PXX]<sub>3</sub>I<sub>3</sub>. A and B are crystallographically independent molecules.

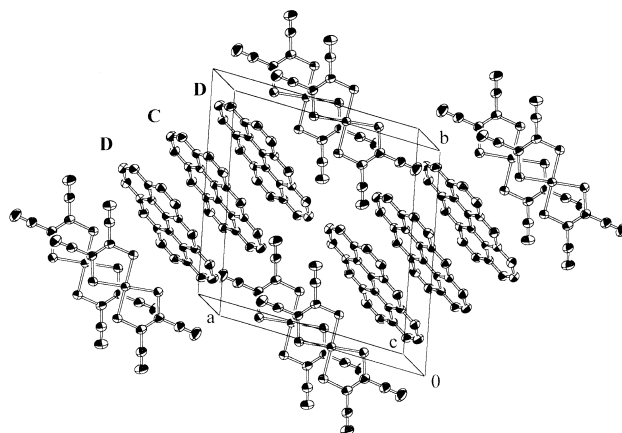
posed of one-dimensional columns of PXX with ·B–A–B–A–B· sequence and discrete I<sub>3</sub> anions. The B–A overlap mode is equal to the A–B mode, while the B–B overlap mode is different from them. The interplanar spacing between A and B (3.385 Å) is shorter than that between B and B (3.422 Å). These differences result in a large difference in the overlap integral (*s*); *s* = 13.0 × 10<sup>-3</sup> for the A–B overlap and 2.13 × 10<sup>-3</sup> for the B–B overlap. The trimeric deformation divides the one-dimensional band for uniformly stacked structure into three subbands. When the trimer accommodates one electron (or one hole in this case), one subband becomes half-filled. If the on-site Coulomb repulsion energy (*U*) is sufficiently small, the material becomes metallic. However, if *U* is rather large, the half-filled band further splits into one filled band and one empty band with an appreciable energy gap between them. This situation is assumed to occur in [PXX]<sub>3</sub>I<sub>3</sub> because of its semi-conducting property.

**Infrared and Vis-NIR Spectra of [PXX]<sub>3</sub>[Ni(mnt)<sub>2</sub>]<sub>2</sub>.** The IR spectrum is shown in Fig. 2(f). The spectrum is complicated due to the contribution from both two chemical species. The important feature is the CN stretching band at 2207 cm<sup>-1</sup>, which has been reported to be a marker band of the formal charge on the [Ni(mnt)<sub>2</sub>] unit.<sup>12</sup> As this band is observed at the same position as that in the spectrum of Bu<sub>4</sub>N[Ni(mnt)<sub>2</sub>] (Fig. 2(c)), the formal charge on [Ni(mnt)<sub>2</sub>] can be assigned as -1. The formal charge on PXX is thus +2/3.

The vis-NIR spectrum is rather similar to that of [PXX]<sub>3</sub>I<sub>3</sub> except for the additional hump due to [Ni(mnt)<sub>2</sub>]<sup>-</sup>, as shown in Fig. 3(d). There are again bands around 11000 cm<sup>-1</sup>, which can be assigned to the PXX cation radical.

The crystal is a poor conductor (10<sup>4</sup>–10<sup>5</sup> Ω cm at room temperature), which is consistent with the crystal structure (*vide infra*).

**Crystal Structure of [PXX]<sub>3</sub>[Ni(mnt)<sub>2</sub>]<sub>2</sub>.** The crystal structure is shown in Fig. 6. In this crystal, again there are two crystallographically independent PXX's; one (molecule C) lies on the inversion center and the other (molecule D) at the general position. The resultant D–C–D trimers are rather isolated in the lattice; the [Ni(mnt)<sub>2</sub>] dimers are inserted between the PXX

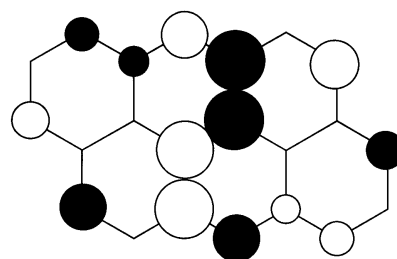
Fig. 6. Crystal structure of [PXX]<sub>3</sub>[Ni(mnt)<sub>2</sub>]<sub>2</sub>. C and D are crystallographically independent molecules.

trimers. Since the  $[\text{Ni}(\text{mnt})_2]$  unit holds a charge  $-1$ , three PXX molecules share the charge  $+2$ . As discussed in the next section, there appear to be some geometrical differences between C and D, meaning that the charge disproportionation occurs within the trimer to some extent.

**Comparison of the Molecular Geometry of PXX.** The bond lengths of PXX in the complexes studied and in  $[\text{PXX}][\text{TCNQ}]$  are summarized in Table 2. The formal charge of PXX in  $[\text{PXX}][\text{TCNQ}]$  was estimated to be about 0.1 from the molecular geometry of TCNQ.<sup>2</sup> Though the accuracy in the PXX crystal is relatively poor due to the small reflection number, the bond lengths are in good agreement with those in  $[\text{PXX}][\text{TNP}]_2$ . The bond lengths in  $[\text{PXX}][\text{TNP}]_2$  are thus more reliable as the data for neutral PXX. For  $[\text{PXX}]_3\text{I}_3$  and  $[\text{PXX}]_3[\text{Ni}(\text{mnt})_2]_3$ , the values are averaged for two crystallographically independent molecules. In the former salt, the differences are relatively small (see  $\delta_{\text{max}}$  in Table 2). On the other hand, the differences between C and D in the latter salt are found to be much larger (most of  $\delta_{\text{max}}$  values exceed  $\sigma_{\text{max}}$ ). This implies that the charge is not uniformly distributed. The charge distribution is expressed as  $\text{PXX}^{+\rho} \rightleftharpoons (1 - \rho)\text{PXX}^0 + \rho\text{PXX}^{+1}$ , where  $\rho$  is the formal charge (molar fraction of  $\text{PXX}^{+1}$ ). The apparent uniform charge distribution occurs when the resonance between  $\text{PXX}^0$  and  $\text{PXX}^{+1}$  is so fast that only its averaged feature is observable. In  $[\text{PXX}]_3[\text{Ni}(\text{mnt})_2]_3$ , the right-hand-side state has considerably lower potential energy, so that the uneven charge distribution becomes observable. Since the averaged bond lengths in Table 2 correspond to the bond lengths of the hypothetical  $\text{PXX}^{+0.67}$ , we can take these values

for the oxidation state  $+0.67$ .

The schematic diagram of the HOMO coefficients of PXX obtained from the extended Hückel calculation (based on the structural data of  $[\text{PXX}]_3\text{I}_3$ ) is shown in Scheme 1. From the distribution of the HOMO coefficients, it is expected that the bonds  $m$  and  $n$  must be sensitive to the fractional charge on PXX. As shown in Table 2, with increasing the formal charge, the bond  $m$  is lengthened and the bond  $n$  is shortened, which is consistent with each bond character as expected from the HOMO coefficients (bonding for  $m$  and anti-bonding for  $n$ ). These data are plotted in Fig. 7 (for  $\text{PXX}^0$ , data of  $[\text{PXX}][\text{TNP}]_2$  are adopted). Linear correlation with similar slopes but opposite signs can be seen. Though the bond  $b$  also shows some correlation that is consistent with the HOMO coefficients, the sensitivity is less. The other bond lengths are nearly constant or irregularly changed by the formal charge. From the fit in Fig. 7, we can deduce the relation between the formal charge  $\rho$  and the bond lengths at  $m$  and  $n$ ,  $d_m$  and  $d_n$  in



Scheme 1.

Table 2. Averaged<sup>a)</sup> Bond Length ( $d$ , Å), Maximum Standard Deviation ( $\sigma_{\text{max}}$ ,  $\times 10^3$  Å), and Maximum Deviation from the Average Value ( $\delta_{\text{max}}$ ,  $\times 10^3$  Å) of PXX

Bond	$d$ ( $\sigma_{\text{max}}^{\text{b)}$ , $\delta_{\text{max}}^{\text{c)}$ )				
	$\text{PXX}^0$ (PXX)	$\text{PXX}^0$ ( $[\text{PXX}][\text{TNP}]_2$ )	$\text{PXX}^{+0.1}$ ( $[\text{PXX}][\text{TCNQ}]$ ) <sup>d)</sup>	$\text{PXX}^{+0.33}$ ( $[\text{PXX}]_3\text{I}_3$ )	$\text{PXX}^{+0.67}$ ( $[\text{PXX}]_3[\text{Ni}(\text{mnt})_2]_3$ )
<b>a</b>	1.391(9, 12)	1.391(3, -)	1.394(2, -)	1.392(4, 4)	1.390(2, 8)
<b>b</b>	1.390(9, 9)	1.386(3, -)	1.382(2, -)	1.381(4, 4)	1.377(2, 17)
<b>c</b>	1.40(10, 20)	1.397(3, -)	1.399(3, -)	1.396(5, 6)	1.398(3, 3)
<b>d</b>	1.37(10, 30)	1.367(3, -)	1.365(3, -)	1.369(5, 7)	1.377(3, 7)
<b>e</b>	1.42(10, 20)	1.426(3, -)	1.418(3, -)	1.427(5, 1)	1.423(3, 4)
<b>f</b>	1.42(10, 60)	1.410(3, -)	1.414(3, -)	1.411(5, 6)	1.408(3, 8)
<b>g</b>	1.37(10, 10)	1.373(3, -)	1.357(3, -)	1.373(6, 4)	1.371(3, 5)
<b>h</b>	1.41(10, 20)	1.402(4, -)	1.401(3, -)	1.402(6, 7)	1.399(3, 9)
<b>i</b>	1.37(10, 30)	1.362(3, -)	1.362(3, -)	1.365(5, 6)	1.374(3, 7)
<b>j</b>	1.412(9, 17)	1.418(3, -)	1.412(3, -)	1.415(5, 4)	1.408(3, 5)
<b>k</b>	1.41(10, 50)	1.414(3, -)	1.416(3, -)	1.410(5, 4)	1.413(3, 2)
<b>l</b>	1.407(9, 27)	1.406(3, -)	1.410(2, -)	1.407(5, 1)	1.412(2, 4)
<b>m</b>	1.366(9, 29)	1.371(3, -)	1.375(2, -)	1.380(4, 3)	1.385(2, 14)
<b>n</b>	1.425(3, -)	1.427(4, -)	1.426(3, -)	1.424(6, 7)	1.413(3, 16)

a) Under centrosymmetric conditions. b) The value of the maximum  $\sigma$  among the bonds averaged. c) The value of the maximum difference from the average value among the bonds averaged. d) Ref. 2.

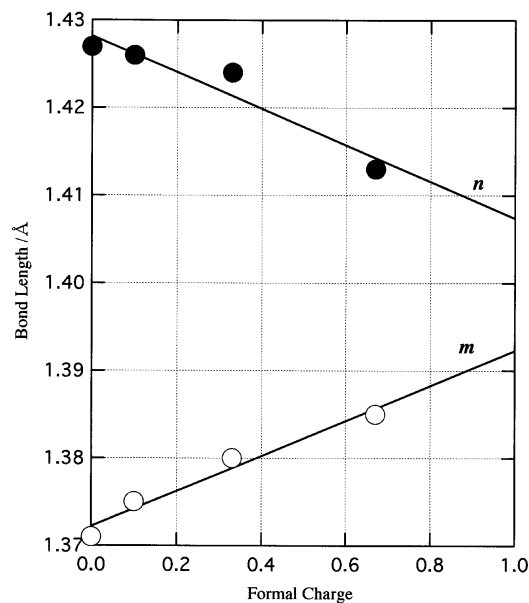


Fig. 7. Bond length (*m* and *n* in Table 2) vs. formal charge plot of PXX.

Å, as follows;

$$\rho = 1.370 - 24.46 \times (d_n - d_m), \quad 0 \leq \rho \leq 1.$$

For other donors or acceptors, the frequency shifts of some specific vibrational modes are utilized for the estimation of the formal charge. However, application of this method is rather limited, since the band has to be well separated from the other bands and can be assigned undoubtedly. In the case of PXX, the bands which are expected to be sensitive to the formal charge (vibrations accompanied by the motion of atoms with the large HOMO coefficients) all lie in the finger print region. For such a situation, molecular geometry is a more powerful index of the formal charge.

In conclusion, the single crystals of three new complexes of

PXX have been prepared and structurally characterized. Some correlation between the bond length and the formal charge on PXX has been observed, and the trend of the bond length change has been found to be consistent with that expected from the HOMO coefficient distribution.

This work was partly supported by a Grant-in-Aid for Scientific Research from the Ministry of Education, Science, Sports and Culture.

## References

- 1 T. J. Kistenmacher, T. J. Emge, A. N. Bloch, and D. O. Cowan, *Acta Crystallogr., Sect. B*, **38**, 1193 (1982).
- 2 M. Hjorth, N. Thorup, P. Frederiksen, and K. Bechgaard, *Acta Chem. Scand.*, **48**, 139 (1994).
- 3 S. Takano, T. Naito, and T. Inabe, *Chem. Lett.*, **1998**, 1249.
- 4 K. Morimoto and T. Inabe, *J. Mater. Chem.*, **5**, 1749 (1995).
- 5 R. Pummerer, E. Prell, and A. Rieche, *Ber. Dtsch. Chem. Ges.*, **59**, 2159 (1926).
- 6 G. Bähr and G. Schleitner, *Chem. Ber.*, **90**, 438 (1957); A. Davison, N. Edelstein, R. H. Holm, and A. H. Maki, *Inorg. Chem.*, **2**, 1227 (1963).
- 7 Unpublished results. The unit cell is monoclinic and the cell dimensions are  $a = 42.650(7)$ ,  $b = 7.583(7)$ ,  $c = 3.814(10)$  Å, and  $\beta = 92.53(10)^\circ$ .
- 8 SIR92: A. Altomare, M. C. Burla, M. Camalli, M. Cascarano, C. Giacovazzo, A. Guagliardi, and G. Polidori, *J. Appl. Crystallogr.*, **27**, 435 (1994).
- 9 "teXsan: Crystal Structure Analysis Package," Molecular Structure Corporation (1985 & 1992).
- 10 Tables of atomic coordinates, anisotropic thermal parameters for non-hydrogen atoms, bond lengths and angles are deposited as Document No. 74010 at the Office of the Editor of *Bull. Chem. Soc. Jpn.*
- 11 J. B. Torrance, J. E. Vazquez, J. J. Mayerle, and V. Y. Lee, *Phys. Rev. Lett.*, **46**, 253 (1981).
- 12 S. P. Best, S. A. Ciniawsky, R. J. H. Clark, and R. C. S. McQueen, *J. Chem. Soc., Dalton Trans.*, **1993**, 2267.